Plant Biotechnology Journal
Open Access

Plant Biotechnology Journal (2022), pp. 1–12 doi: 10.1111/pbi.13958

Development of a 135K SNP genotyping array for *Actinidia arguta* and its applications for genetic mapping and QTL analysis in kiwifruit

Ran Wang[1,2], Siyuan Xing[3], Peter M. Bourke[2], Xiuquan Qi[1], Miaomiao Lin[1], Danny Esselink[2], Paul Arens[2], Roeland E. Voorrips[2], Richard G.F. Visser[2], Leiming Sun[1], Yunpeng Zhong[1], Hong Gu[1], Yukuo Li[1], Sikai Li[1], Chris Maliepaard[2,*] and Jinbao Fang[1,*]

[1]*Zhengzhou Fruit Research Institute, Chinese Academy of Agricultural Sciences, Zhengzhou, China*
[2]*Plant Breeding, Wageningen University & Research, Wageningen, The Netherlands*
[3]*Animal Breeding and Genomics, Wageningen University & Research, Wageningen, The Netherlands*

Received 9 August 2022;
revised 22 October 2022;
accepted 31 October 2022.
**Correspondence* (Tel +8637165330995; email fangjinbao@caas.cn (J.F.)
Tel +31317480855; email chris.maliepaard@wur.nl (C.M.))

Keywords: kiwifruit, SNP array, polyploid genetics, genetic linkage map, QTL analysis.

Summary

Kiwifruit (*Actinidia* spp) is a woody, perennial and deciduous vine. In this genus, there are multiple ploidy levels but the main cultivated cultivars are polyploid. Despite the availability of many genomic resources in kiwifruit, SNP genotyping is still a challenge given these different levels of polyploidy. Recent advances in SNP array technologies have offered a high-throughput genotyping platform for genome-wide DNA polymorphisms. In this study, we developed a high-density SNP genotyping array to facilitate genetic studies and breeding applications in kiwifruit. SNP discovery was performed by genome-wide DNA sequencing of 40 kiwifruit genotypes. The identified SNPs were stringently filtered for sequence quality, predicted conversion performance and distribution over the available *Actinidia chinensis* genome. A total of 134 729 unique SNPs were put on the array. The array was evaluated by genotyping 400 kiwifruit individuals. We performed a multidimensional scaling analysis to assess the diversity of kiwifruit germplasm, showing that the array was effective to distinguish kiwifruit accessions. Using a tetraploid F1 population, we constructed an integrated linkage map covering 3060.9 cM across 29 linkage groups and performed QTL analysis for the sex locus that has been identified on Linkage Group 3 (LG3) in *Actinidia arguta*. Finally, our dataset presented evidence of tetrasomic inheritance with partial preferential pairing in *A. arguta*. In conclusion, we developed and evaluated a 135K SNP genotyping array for kiwifruit. It has the advantage of a comprehensive design that can be an effective tool in genetic studies and breeding applications in this high-value crop.

Introduction

Recent advances in high-throughput SNP array technologies provide a powerful platform for genotyping SNPs across the genome of organisms, owing to their effectiveness in terms of cost per marker, especially for polyploids. Various SNP genotyping arrays have been developed in polyploid crops, such as strawberry, rose, potato, wheat and chrysanthemum (Bassil *et al.*, 2015; Koning-Boucoiran *et al.*, 2015; van Geest *et al.*, 2017; Vos *et al.*, 2015; Winfield *et al.*, 2016). These arrays contain a large number of SNPs and have been demonstrated to be effective tools for linkage analysis, QTL mapping of important traits and genome-wide association analysis (Allen *et al.*, 2017; Bourke *et al.*, 2018b; Vos *et al.*, 2015; Vukosavljev *et al.*, 2016; You *et al.*, 2018). The SNP array approach has the advantages of cost-efficiency, low error rates, high density and ease of automation of data processing. In addition, allele dosages can be assigned to individuals relatively easily by available tools using the relative strength of two allele-specific signals (Serang *et al.*, 2012; Voorrips *et al.*, 2011). However, it also has the disadvantage that only a fixed set of SNPs can be evaluated, making it less flexible than sequencing-based approaches.

Kiwifruit is an economically important crop with an annual worldwide production of 4.34 million tons (FAOSTAT, 2019, http://www.fao.org/faostat/), despite its relatively short history of domestication since the early 20th century (Ferguson, 2013). Kiwifruit is a woody, perennial and deciduous vine, which belongs to the genus *Actinidia*. It is comprised of 54 species with very diverse morphological and genetic characteristics (Testolin *et al.*, 2016). It also naturally occurs in a wide range of ploidy levels, from diploid (2x) to dodecaploid (12x). Global kiwifruit production is mainly dominated by polyploid kiwifruit cultivars, which have the advantage of possessing large fruits and displaying strong disease resistance (Ferguson, 2013; Tahir *et al.*, 2020; Wu *et al.*, 2012). The global kiwifruit market is dominated by the yellow-fleshed *A. chinensis* var. *chinensis* (either diploid or tetraploid) and the green-fleshed *A. chinensis* var. *deliciosa* (hexaploid). Over the last decade, there has been increasing interest in the commercialization of *Actinidia arguta*,

Please cite this article as: Wang, R., Xing, S., Bourke, P M., Qi, X., Lin, M., Esselink, D., Arens, P., Voorrips, R E., Richard G.F.Visser, Sun, L., Zhong, Y., Gu, H., Li, Y., Li, S., Maliepaard, C. and Fang, J. (2022) Development of a 135K SNP genotyping array for *Actinidia arguta* and its applications for genetic mapping and QTL analysis in kiwifruit. *Plant Biotechnol J.*, https://doi.org/10.1111/pbi.13958.

also known as kiwiberry. Multiple ploidy levels occur in this species, but most selections are tetraploid (Zhang *et al*., 2017).

In addition to this variation in ploidy, *Actinidia* species are mostly functionally dioecious. Usually, female plants from germplasm collections have been extensively characterized, but this is not the case for male plants with no fruiting, for which the contribution to aspects of fruit production and fruit quality is difficult to evaluate. It requires a large investment in cost and time for breeders, as multiple experimental crosses of a male tester are needed for progeny testing. Phenotypic selection is still the primary breeding method used by kiwifruit breeders. Phenotypic traits such as fruit quality and *Pseudomonas syringae* pv. *Actinidiae* resistance are mostly quantitative, genetically controlled by multiple genes and with a large influence from both cultivation management and the growing environment (Tahir *et al*., 2019, 2020; Testolin *et al*., 2016). The genetic basis of these traits is complex in dioecious polyploids, making the breeding for desired traits even more challenging.

Kiwifruit production has continuously grown over the last decade, but to increase breeding efficiency and reduce breeding cycles, better knowledge is required regarding genes and genomic regions involved in agronomically important traits. Various types of molecular markers have been developed in kiwifruit for the genetic mapping of commercially important traits (Fraser *et al*., 2009; Scaglione *et al*., 2015). For instance, the first genetic maps were constructed in a diploid *A. chinensis* × *A. callosa* interspecific population using a limited number of markers, including amplified fragment length polymorphisms (AFLPs) and simple sequence repeats (SSRs) (Testolin *et al*., 2001). The first draft genome of a diploid kiwifruit *A. chinensis* was released in 2013, which has facilitated genome-wide variant detection and the development of dedicated molecular tools (Huang *et al*., 2013). For polyploid kiwifruit, a genetic map was recently constructed using SNPs for mapping several fruit quality traits in hexaploid kiwifruit (Popowski *et al*., 2021). However, using a genotyping-by-sequencing (GBS) approach, only simplex × nulliplex markers could be used in that study due to insufficient read depth to accurately call more complex marker types, resulting in a lower map density.

With an objective to utilize SNPs for kiwifruit improvement, we developed a high-density SNP genotyping array using 135K SNPs identified across multiple kiwifruit species. The array was evaluated by a set of germplasm accessions and a tetraploid *A. arguta* population. We constructed an integrated linkage map of 29 linkage groups and performed QTL mapping for the sex locus in *A. arguta*. We demonstrate that the kiwifruit 135K SNP array is useful for genomic analysis and genetic mapping of important traits, which is of great importance for research as well as breeding applications.

Results

Development of the kiwifruit 135K SNP array

A germplasm panel of 40 kiwifruit genotypes was sequenced for genome wide SNP discovery, including cultivated species (*Actinidia arguta* var. *arguta, A. chinensis* var. *chinensis*, *A. chinensis* var. *deliciosa* and *A. eriantha*) and wild species (*A. arguta* var. *purpurea*, *A. macrosperma*, *A. polygama* and *A. valvata*), shown in Figure 1a and Table S1. Our aim was to identify SNPs that can be used for a wide range of kiwifruit genotypes as well as for genetic mapping in the tetraploid *A. arguta* F1 population specifically. Of the main cultivated species, we identified an average of 11.35M SNPs from *A. chinensis* var. *chinensis*, 20.65 M SNPs from *A. chinensis* var. *deliciosa* and 27.43M SNPs from *A. arguta*. The workflow of the 135K SNP array design is described in Figure 1b. More details of SNP detection, filtering and selection are provided in the experimental procedure. All identified SNPs from sequencing data were filtered, resulting in a dataset of 411 023 SNPs. Putative SNPs and their flanking sequences were assessed by Affymetrix Axiom platform. Following Affymetrix recommendations, we selected 403 335 (recommended and neutral) SNPs for further filtering, which led to 134 729 SNPs tiled on the array. These SNPs are evenly distributed over the genome, with an average of 4645 SNPs per chromosome and an average density of one SNP/4110 bp (Figure 2a). The maximum SNP number was found on Chr23 (5.1%, 6838), while the minimum SNP number was found on Chr4 (2.5%; 3364). Annotation of the Red5 genome showed that 35.2% (47422) of the SNPs were from the introns while 20.0% (26946) of the SNPs were from the exons. The other major groups include SNPs from downstream regions (15.6%, 20 984), upstream regions (15.0%, 20 203), intergenic regions (9.2%, 12 386), UTR_3_prime (3.1%, 4220), UTR_5_prime (1.6%, 2221) and SNPs involved in early termination or elongation of the transcripts (0.18%, 244).

Evaluation of the kiwifruit 135K SNP array

The kiwifruit 135K array was evaluated using 400 kiwifruit individuals, including germplasm accessions and a tetraploid *A. arguta* F1 population, listed in Table S2. The SNP genotyping results from the 134 279 SNPs on the array were classified into six categories: SNPs were monomorphic (Mono High Resolution), or polymorphic (Poly High Resolution); only two clusters were observed (No Minor Homozygote); an additional cluster was observed from the SNPs whose flank sequences were significantly different from the probes (Off-Target Variant); the genotype call rate was below 95% (Call Rate Below Threshold); SNP clustering with issues could not be classified from the above (Other) (Figure 2b); three of these (Poly high resolution, Mono high resolution, No minor homozygote) were assessed as high quality. This resulted in a total number of 81 275 high quality SNPs, of which 69 707 SNPs were polymorphic across *Actinidia* species. In the second attempt, we reanalysed only the *A. arguta* individuals for all SNPs. It resulted in 92 329 high-quality SNPs, of which 75 990 were polymorphic in the species.

To evaluate the efficiency of the kiwifruit 135K array, we selected 93 genotypes from germplasm accessions and the mapping population to perform a multidimensional scaling (MDS) analysis. Genotypes were mainly separated into two groups: Group I is from the *A. arguta* and Group II is from the *A. chinensis* complex and other non-cultivated species (Figure 3a). In Group I, all accessions belonging to *A. arguta* are located at the left of the plot. We observed that accessions such as 'Ruby-3' collected from central China were located at the upper side of the plot, while 'Kuilv-M' and other accessions collected from the northeast of China were located at the bottom of the plot. The F1 progeny were clustered at approximately equal distances from the female parent 'Ruby-3' and the male parent 'Kuilv-M'. Similar results were found for another F1 progeny of cross 'Ruby-3' × '11–17', suggesting the reliability of the relationship and clustering of Group I. In Group II, the *A. chinensis* complex consisting of *A. chinensis* var *chinensis* and *A. chinensis* var *deliciosa* were clustered closely together. The other species (*A. eriantha*, *A.*

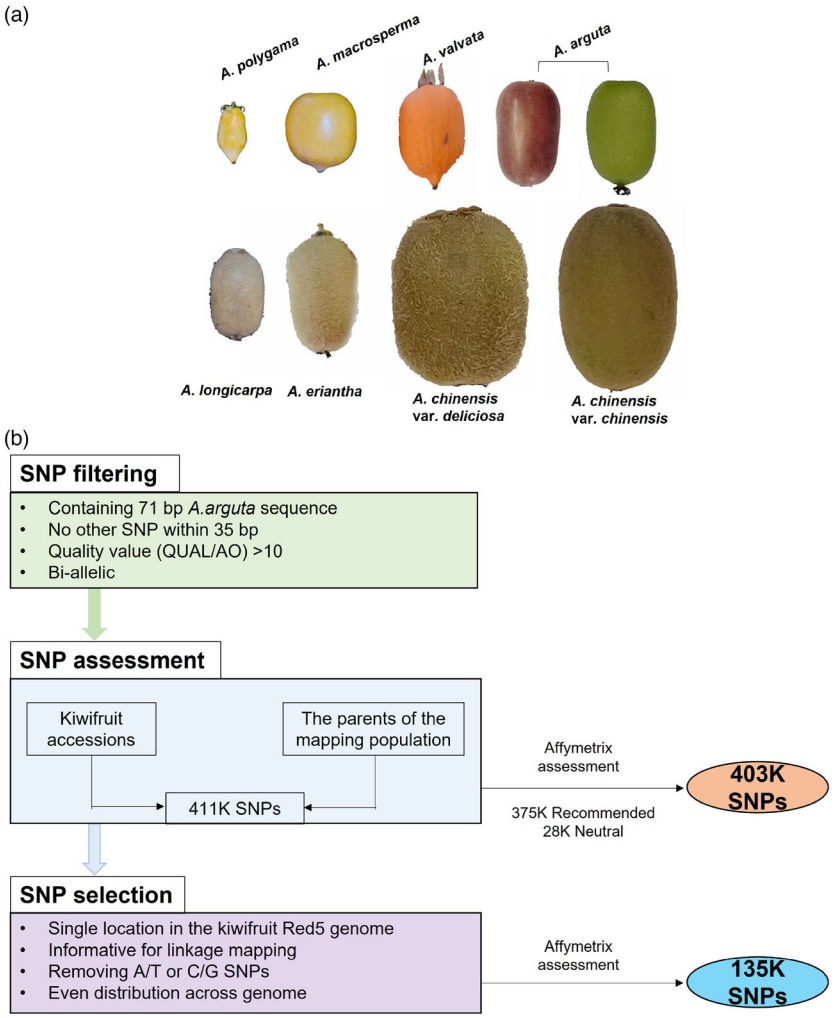

Figure 1 Development and applications of the kiwifruit 135K array (a) Fruit diagram of 8 *Actinidia* species used in the study. (b) Flow diagram shows steps of the development of the 135K genotyping array.

hemsleyana, *A. macrosperma, A. polygama* and *A. valvata*) were scattered outside of the *A. chinensis* complex (Figure 3b).

To assess the suitability of the array for genotyping tetraploids, marker dosages of tetraploid individuals were called based on the signal intensity of the array using fitPoly. The software assigned the markers into one of five dosages: nulliplex (0), simplex (1), duplex (2), triplex (3) and quadruplex (4), by fitting mixture models of five normal distributions to the allele signal ratios. (Voorrips *et al*., 2011; Zych *et al*., 2019). For the array data of 134 729 markers, dosage calling of the tetraploid individuals resulted in 128 580 markers fitted and 6149 rejected by fitPoly. The percentage of missing calls was low, with an average of 2.5% missing calls per genotype and 2.7% missing calls per marker. Genotyping reproducibility across eight replicates was 99.3% on average of the markers called with dosage.

Linkage map construction

Genotypic data generated from the kiwifruit 135K array were used to construct a genetic linkage map for the tetraploid *A. arguta* population of 'Ruby-3' and 'Kuilv-M'. Markers were processed in the R package of polymapR (Bourke *et al*., 2018a), of which 117 917 showed expected segregation to the parental dosages. A principal component analysis of the population identified three pairs of duplicates and four incompatible progenies. Marker dosages were converted into the simplest segregation types of nine fundamental marker classes: simplex × nulliplex (1 × 0), nulliplex × simplex (0 × 1), duplex × nulliplex (2 × 0), nulliplex × duplex (0 × 2), simplex × simplex (1 × 1), simplex × triplex (1 × 3), simplex × duplex (1 × 2), duplex × simplex (2 × 1), duplex × duplex (2 × 2), as shown in Figure S1. This resulted in a final dataset of 77 480 unique markers and a mapping population size of 315 individuals for the construction of a linkage map. We used 1 × 0 and 0 × 1 markers for the initial clustering of 116 homologues of each of the two parents. The homologues were bridged using 2 × 0 and 1 × 1 markers to represent 29 LGs of four homologues. All other types of markers were subsequently assigned to a LG using the linkage with 1 × 0 markers.

After adding back the duplicate markers, we generated an integrated linkage map of 106 945 phased markers covering 3060.9 cM. The average length is 105.5 cM per LG with the maximum gap ranging from 0.4 cM to 4.8 cM. The LGs were numbered according to the corresponding chromosome of the Red5 *A. chinensis* genome by BLAST, where 98 856 marker

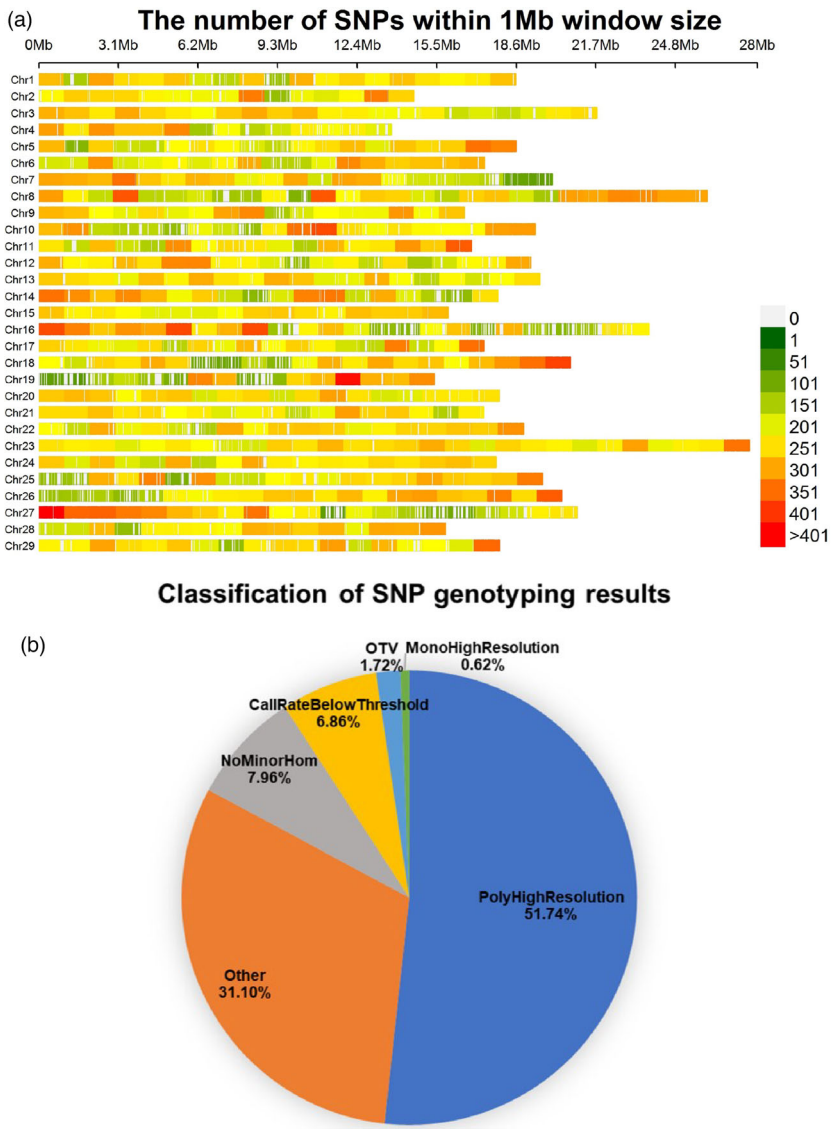

Figure 2 Features of the 135K kiwifruit genotyping array. (a) Density of SNP variants along chromosomes. (b) Classification of SNP genotyping results into six categories. SNPs were monomorphic (Mono High Resolution), or polymorphic (Poly High Resolution); only two clusters were observed (No Minor Homozygote); an additional cluster was observed from the SNPs whose flank sequences were significantly different from the probes (Off-Target Variant = OTV); the genotype call rate was below 95% (Call Rate Below Threshold); SNP clustering with issues could not be classified from the above (Other).

positions derived from the *A. chinensis* genome were assigned to the expected LGs. Several LGs were re-oriented according to the physical map, resulting in the final order and orientation of the markers on the linkage map (Figure 4a). All 29 linkage groups were densely covered with markers and the distribution of the markers mapped on the linkage groups is shown in Table 1. We further compared the genetic position of markers against their physical positions of *A. chinensis* genome by Marey plot, showing a high degree of synteny between *A. arguta* and *A. chinensis* species. For some LGs, we observed some disruptions such as inversions or translocations (Figure 4b). We double-checked the collinearity between the tetraploid *A. arguta* integrated linkage map described here and the previously published diploid *A. chinensis* linkage map (Zhang *et al.*, 2015) (Figure S2).

QTL mapping of the sex locus and estimation of preferential pairing

The phased linkage map was used to reconstruct the inheritance of parental haplotypes by estimating identity-by-descent (IBD) probabilities in the population. The IBD probabilities allow QTL detection across all homologues simultaneously. The flowering of the progenies revealed a 1:1 ratio between male and female offspring. Because we are ultimately interested in fruit traits, we selected 39 males and 266 females as the mapping population. QTL analysis of the sex locus was performed based on IBD probabilities of the population. Initially, a highly significant QTL peak was observed on LG3 at 86 cM, but we noticed that some skewed markers that correlated to the sex ratio of progenies had

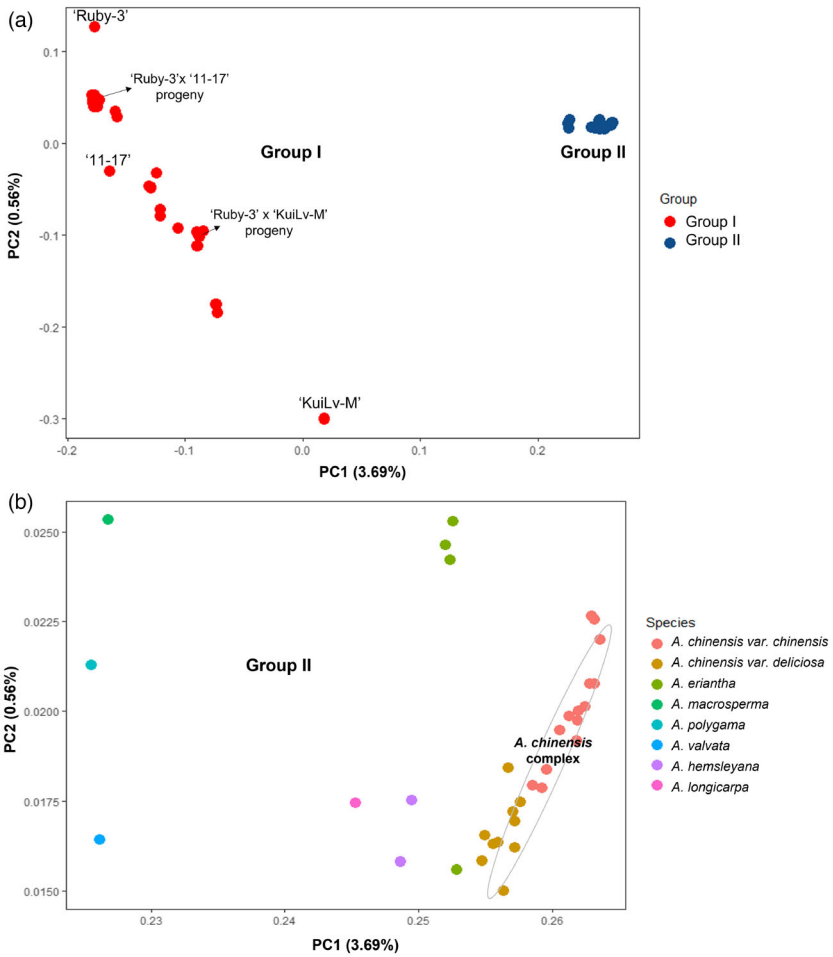

Figure 3 Multidimensional scaling (MDS) analysis of kiwifruit accessions. a) MDS plot of the *Actinidia* species. b) MDS plot of the Group II accessions.

been filtered out before linkage mapping. The sex-linked markers were all mapped to chr3 of the *A. chinensis* genome, then were added to the dataset for re-mapping (Figure S3). In the subsequent QTL scan, a single QTL peak was positioned on LG3 at 82.1 cM with an LOD score of 145.1 (Figure S4). The major effect for maleness was mapped to homologue 8 (our numbering) that was inherited from the male parent (Figure 5). The QTL segregation type is qqqq × qqqQ (Q is the allele for maleness), where male offspring carried the haplotype-specific allele (Figure S5). The male-linked markers were located in the pericentromeric region, which had a corresponding span of 6 Mbp on the *A. chinensis* genome. Seven simplex markers from the QTL region were analysed by PCR amplification and Sanger sequencing, confirming that the male-linked markers were mapped to chr3 via BLAST search.

Furthermore, we investigated the meiotic pairing behaviour of the chromosomes. Under the assumption of bivalent pairing and using the predictions from the Hidden Markov Model, we applied a χ^2 test for deviations from the expected counts assuming random pairing. All possible combinations of pairing are shown in Figure 6, the significant deviations from random pairing were observed on LG15 of the male parent (*P*-value of 2.26×10^{-4}), and none of the other deviations were significant at $P < 0.001$ (Table S3). Our results, therefore, demonstrated that tetraploid *A. arguta* has mostly polysomic inheritance with paternal-specific preferential pairing behaviour on one LG in our population.

Discussion

Development of the kiwifruit 135K SNP array

Since the completion of the kiwifruit draft genome, kiwifruit breeding has gradually shifted from traditional phenotypic selection to selection including markers for some traits (Hale *et al.*, 2018; Tahir *et al.*, 2019; Zhang *et al.*, 2015). This is promising for crops with a long generation time, since marker-assisted selection (MAS) can significantly facilitate the selection process in breeding. For example, early sex identification by male-specific markers in kiwifruit could significantly reduce the costs of plant maintenance in the field (Fraser *et al.*, 2009). The high-throughput genotyping array has been demonstrated to be a valuable tool in genetics and breeding for some perennial crops such as apple, cherry, peach and pear (Chagne *et al.*, 2012; Li *et al.*, 2019; Peace *et al.*, 2012; Verde *et al.*, 2012). The present study is the first attempt to develop a high-throughput genotyping array for kiwifruit. We aimed for an array of high quality to be used for genetic studies and breeding applications in kiwifruit and related species. By sequencing a germplasm collection, we noted that *Actinidia* species are highly heterozygous. The high nucleotide diversity of the genome is a disadvantage in the sense that

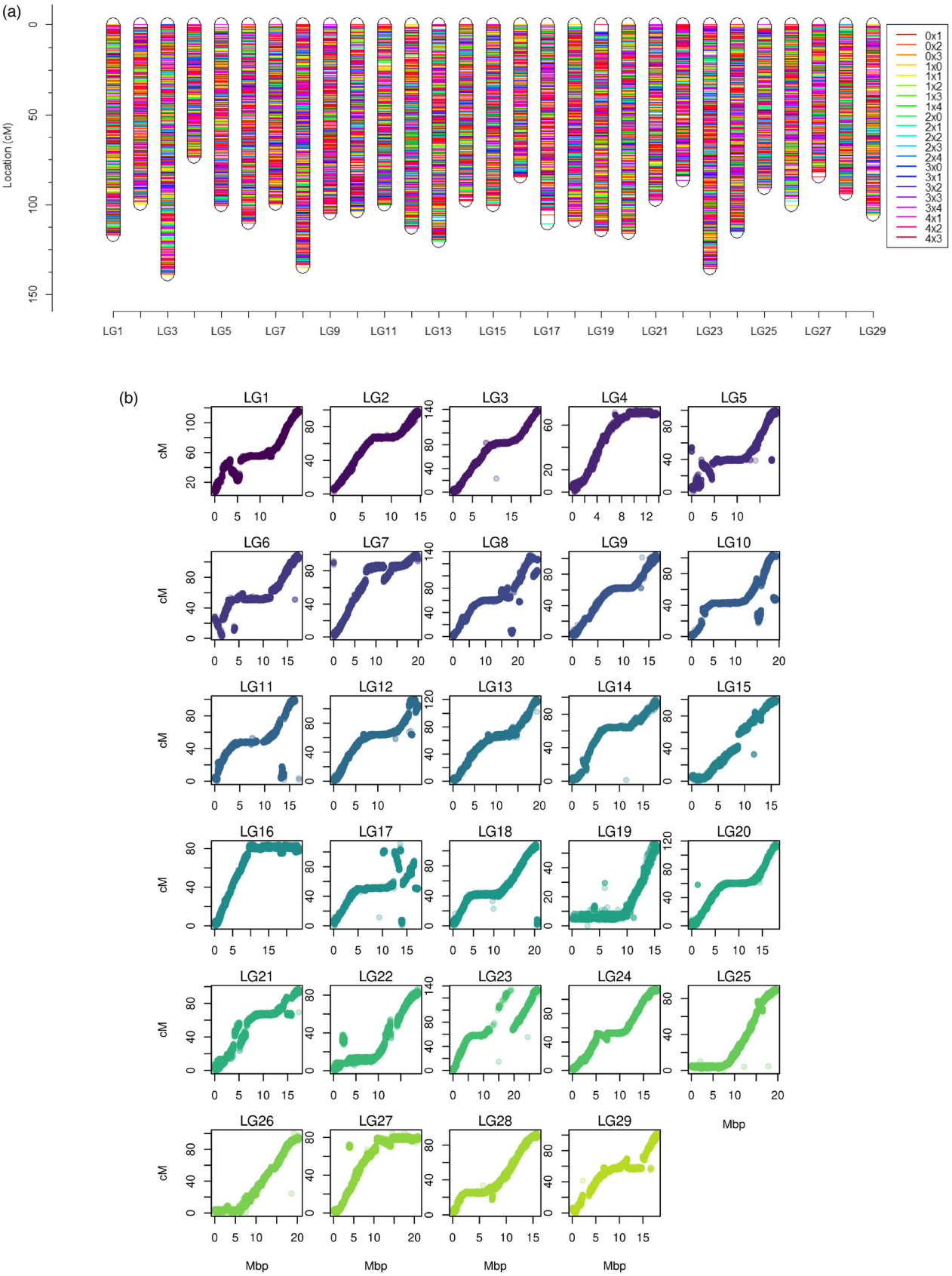

Figure 4 Linkage map construction using array data of a tetraploid *A. arguta* population. (a) Integrated linkage map of all 29 LGs for the tetraploid F1 population, with marker segregation types highlighted. (b) Comparison of the genetic map with the diploid kiwifruit Red5 genome. Marker positions on the genetic map were plotted against their Mbp position on the physical map.

Table 1 Statistics of the phased linkage map of the tetraploid population 'Ruby-3' × 'Kuilv-M'

Linkage group	Length (cM)	Phased markers
LG1	117.2	3951
LG2	99.9	3375
LG3	139.0	3591
LG4	73.6	2635
LG5	100.4	3555
LG6	110.3	3970
LG7	99.5	4073
LG8	134.8	4738
LG9	105.0	3250
LG10	104.0	3806
LG11	100.2	2957
LG12	112.8	3944
LG13	120.6	3794
LG14	97.7	3493
LG15	100.4	3683
LG16	84.7	4283
LG17	110.8	3212
LG18	109.1	3989
LG19	114.3	4548
LG20	115.8	3476
LG21	97.5	3433
LG22	86.8	3508
LG23	135.5	3892
LG24	115.0	3285
LG25	90.9	3896
LG26	100.6	3853
LG27	84.6	4009
LG28	93.9	3403
LG29	105.9	3343
Total	**3060.9**	**106 945**

the flanking SNPs can result in failed assays (Vos *et al.*, 2015). Taking into consideration the cost-effectiveness and future applications of the array, we targeted it for polyploid kiwifruit species. Having multiple copies of each homologue, specialized genotype calling approaches are required to assign allele dosages in polyploids. Though sequencing-based approaches are an alternative for SNP polymorphism detection, the accuracy of allele dosage estimates is dependent on the read counts which are linked to the sequencing depth (Gerard *et al.*, 2018). Deep sequencing leads to a high cost of genotyping a large number of individuals while it is still difficult to clearly distinguish between different heterozygotes differing in the dosages of the alleles (Uitdewilligen *et al.*, 2013). Moreover, the huge amount of data generated by deep sequencing requires advanced bioinformatic skills and considerable computational resources for data analysis (Bajgain *et al.*, 2016). With this, we developed a high-density array and described a workflow that overcomes the challenges of genome diversity and polymorphism density in kiwifruit. It involved a number of steps, for example, re-mapping of reads to a modified genome improved the sequence specificity to *A. arguta*. This strategy avoided sequence variation in the immediate proximity of target SNPs to reduce interference of flanking SNPs.

Application of the kiwifruit 135K SNP array

Although the number of accessions in the germplasm panel was small, the evaluation of the array with these 93 genotypes demonstrated its value for germplasm analysis of this high-value crop. The overall population structure observed within *A. arguta* genotypes may be explained by geographical origin. Genotypes from central China and northeast China clustered separately in the MDS plot. The cluster of *A. chinensis var chinensis* and *A. chinensis var deliciosa* is explained less well by geographical origin, perhaps due to inconsistency between geographical origin and registration location of the cultivars, as well as the frequent exchange of materials during breeding activities. The cluster of the *A. chinensis* complex further proves that the genetic backgrounds of the main cultivars are very narrow, we thus propose that interspecific hybridization may give extra genetic variation and potential for breeding in this dioecious crop.

Kiwifruit has a large basic chromosome number of x = 29, which is clearly a disadvantage for genetic mapping in polyploid kiwifruit. Constructing a linkage map for such a polyploid crop is always challenging due to the complexity of distinguishing

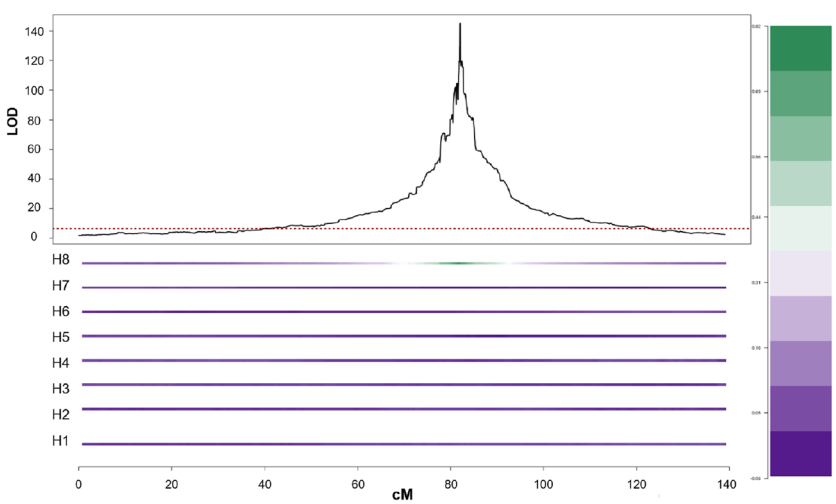

Figure 5 QTL analysis of the sex locus at LG3. Colours link the homologue effects at the QTL peak on showing paternal homologue 8 is associated with male progeny. Maternal homologues are numbered H1–H4 while paternal homologues are numbered H5–H8. Positive effects are coloured green, while negative effects are coloured purple.

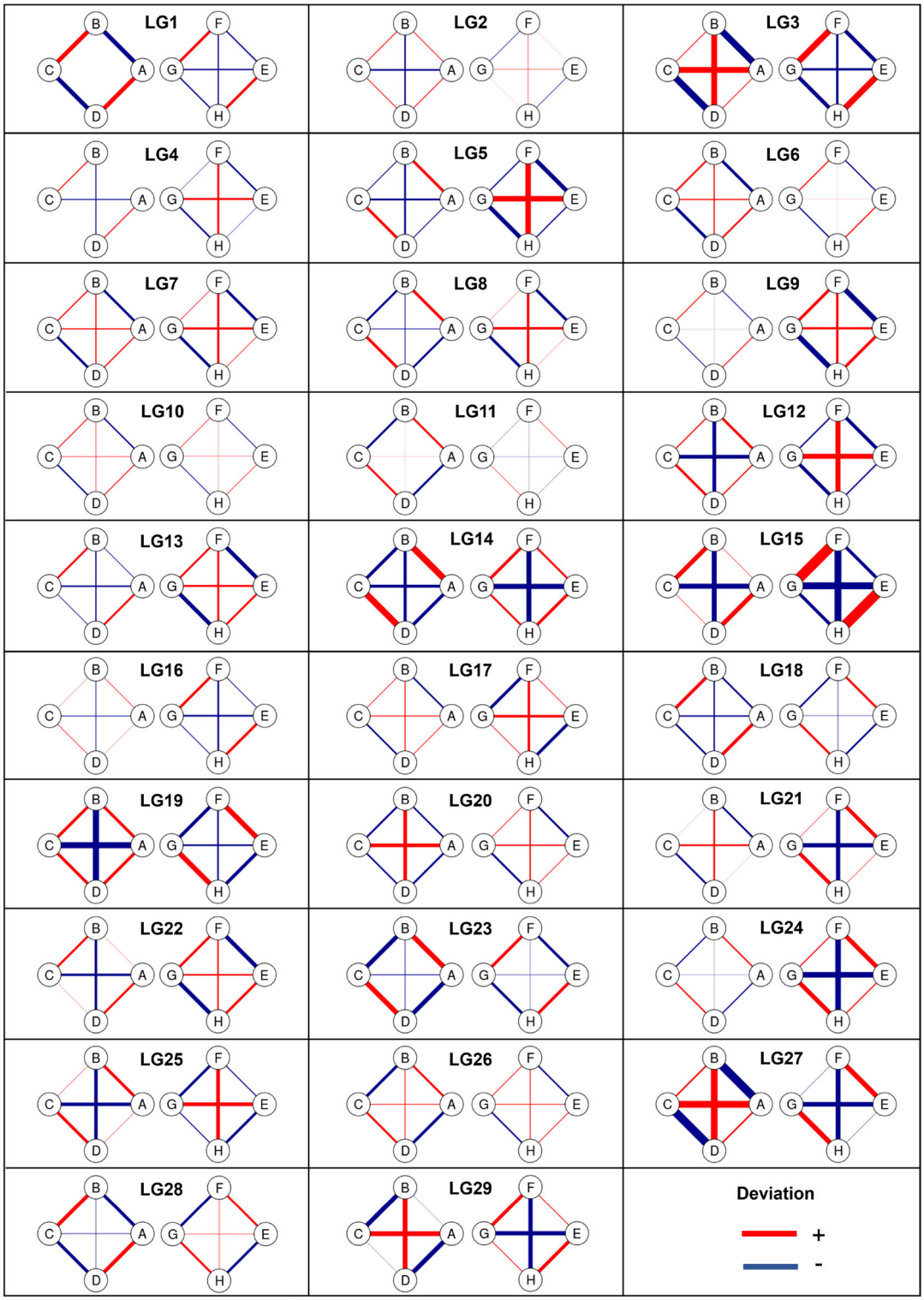

Figure 6 Visualization of pairing behaviour of parental homologues in the tetraploid F1 population. Maternal homologues are labelled A–D, paternal homologues are labelled E–H. The width of the line represents the magnitude of deviations from a random pairing model. An excess of pairing counts is coloured red and a lack of counts is coloured blue.

between homologue linkage groups and chromosomal linkage groups. In this study, one of the benefits of our array design strategy is that it provided a large pool of markers that were segregating in the tetraploid *A. arguta* population, with even genome coverage for all chromosomes and homologues. We mapped 106 945 markers allowing homologue maps to be integrated per chromosome, which to the best of our knowledge is the highest density linkage map in the genus *Actinidia*

published to date. Our linkage map has a good pattern with high visibility of the chromosome arms and centromere on the Marey plots, showing of high-quality linkage map constructed. Assigning the *A. arguta* linkage groups to *A. chinensis* chromosomes also revealed a high level of synteny at the chromosomal level between these species. There are very few deviating syntenic regions scattered across the linkage map, these could be due to either the misplaced on the physical map, or different locations across species. For example, the Marey plots indicated an inversion of 20 cM on LG1 of *A. arguta*, this is more likely to be an assembly error as the inversion was also observed in a separate genetic mapping study in tetraploid *A. chinensis* (Tahir *et al*., 2020).

Dioecy occurs only in 6% of angiosperms (Renner, 2014). The genetic basis of dioecy in *Actinidia* species has been well-established as a heterogametic XY system (Fraser *et al*., 2009). This is supported by the evidence of the 1:1 male-to-female sex ratios in wild and most controlled crosses at different ploidy levels (Fraser *et al*., 2009; Testolin *et al*., 2016). In this study, the first genetic mapping of the sex locus in tetraploid *A. arguta* is presented, revealing a single, major-effect simplex QTL allele associated with sex on LG3. The large population size and trait heritability in the analysis provide high power for the detection of the QTL associated with sex. The GIC is a measure of how much information is captured by marker data and it is one of the most important factors for successful QTL mapping (Bourke *et al*., 2019). The GIC profiles of linkage groups determined per homologue indicate that our dataset was high quality (Figure S6). BLAST results of flanking sequences of the LG3 markers rules out the possibility that the markers aligned to multiple positions in the genome. Furthermore, the cluster of male-linked markers appears to be located in or very close to the centromere of LG3. In contrast, previous genetic mapping studies have mapped the sex-determining region (SDR) to the subtelomeric region of LG25 in an interspecific population of *A. rufa* × *A. chinensis*, as well as a tetraploid *A. chinensis* var. *chinensis* population (Tahir *et al*., 2020; Zhang *et al*., 2015). Two sex-determining genes have been identified: *Shy Girl* acts as a dominant suppressor of carpel development, while *friendly boy* acts as a male promoting factor for male fertility (Akagi *et al*., 2019). Recent genome assembly of a male kiwifruit has confirmed that both genes are located in the SDR of chromosome 25 (Tahir *et al*., 2022).

According to the evidence presented here, it is likely that the chromosome carrying the SDR differs between *Actinidia* species with alternate chromosomal regions containing the sex-determining loci. Possible causes, such as independent evolution of the SDR or translocational rearrangement, for such differences, have been described in plants (Wei *et al*., 2017). In *Populus*, inconsistencies of heterogametic sex and location of the sex locus have been established via comparative mapping (Paolucci *et al*., 2010). Male heterogamety was observed in *Populus tremula* and *Populus tremuloides*, whereas both male and female heterogamety were observed in *Populus alba* (Pakull *et al*., 2011). The SDR in *P. tremuloides* resides in a pericentromeric region of LG19 that differs from other species (where it has been mapped to more terminal regions of the chromosome). In strawberries, a conserved SDR cassette has repeatedly changed genomic location across multiple octoploid *Fragaria* taxa , with the accumulation of the SDR adjacent sequence and increase of the SDR size. This supports a hypothesis of a "move-lock-grow" mechanism for the expansion and diversity of sex chromosomes (Tennessen *et al*., 2018). Further, dioecy can be associated with polyploidy in angiosperms (Glick *et al*., 2016). Polyploidization is possibly accompanied by genome restructuring due to whole-genome duplication or genomic recombination, this may then contribute to the translocation of the SDR. It is also possible that extensive hybridizations during evolution facilitate the diversity in sex linkage within the *Actinidia* genus, in which frequent hybridization has occurred in the wild, with rapid reticulate radiation being influenced by geographical patterns of distribution (Liu *et al*., 2017).

Investigating meiotic pairing will help us to better understand the mode of inheritance in these polyploids. Here, we found some evidence of parent-specific preferential pairing on LG15 in the male parent, whereas the other LGs showed no significant deviations from tetrasomic behaviour. This is broadly consistent with the previous finding reported in a tetraploid *A. chinensis var. chinensis* population, where preferential pairing was detected on LG20, LG23 and LG27 in the female parent and LG7, LG15, LG22 and LG27 in the male parent (Tahir *et al*., 2020). Interestingly, both studies concur regarding non-random pairing on male LG15. Together, these studies provide solid evidence to classify tetraploid kiwifruit as showing mostly tetrasomic inheritance with incidental partial preferential pairing occurring on some chromosomes. Further, these results also suggest that the partial preferential pairing is genus-wide rather than population-specific in *Actinidia*. Further studies to elaborate on the mechanism of preferential pairing on the indicated chromosome would be of particular interest, it may give an indication of the complex breeding history.

In summary, we screened a germplasm collection to identify SNPs across *Actinidia* species, filtered and selected 135K SNPs to develop a high-genotyping kiwifruit array. The array has been used to genotype kiwifruit individuals and showed very effective to distinguish kiwifruit accessions. Furthermore, for a tetraploid *A. arguta* population, we generated a high marker density integrated linkage map of 29 LGs and performed QTL analysis for the sex locus that led to the identification of a novel QTL on LG3. Our study points to diversity in sex linkage within the *Actinidia* genus, providing new insights into sex determination in the genus that can also be exploited for early assessment of plant gender in breeding programs. We finally presented evidence to support tetrasomic inheritance with partial preferential pairing in kiwifruit. In conclusion, the kiwifruit 135K array is useful for genome-wide genetics studies and breeding applications in polyploid kiwifruit.

Experimental procedures

Plant materials

A germplasm panel of 40 kiwifruit genotypes was selected for sequencing, including cultivated species and wild species (Table S1). The panel also included the parents 'Ruby-3' (female) and 'KuiLv-M' (male) of a tetraploid *A. arguta* F1 population. To evaluate the 135K array, the panel of 40 kiwifruit germplasm genotypes, additional germplasm genotypes and the F1 population of 'Ruby-3' × 'Kuilv-M' (in total 400 individuals) were genotyped using the array (Table S2). For the F1 population, we preferably included female plants, accounting for 84–88% of the mapping population (10 plants sex unknown) used in the genetic analysis. Plants were grown at the Zhengzhou Fruit Research Institute, China, under standard field management.

SNP detection and selection

Genomic DNA was extracted from frozen young leaves using Plant DNA Extraction Kit (Tiangen Biotech Co., Ltd., Beijing, China). Paired-end DNA sequencing libraries were prepared as

recommended by the manufacturer protocols and sequenced on Illumina Novaseq platform (Illumina, San Diego, CA, USA). Reads were aligned to the kiwifruit (*A. chinensis* var. *chinensis*) Red5 genome using bwa-mem (version 0.7.15) (Pilkington *et al*., 2018). Read duplicates were removed using Picard and SNPs were identified by freebayes with tetraploid settings.

For an Axiom array, it is recommended to design the probe 16–35 bp upstream or downstream of the variants. Due to the high level of heterozygosity and polyploidy of the *A. arguta* genotypes, it proved difficult to design probes without the interference of variants in the flanking sequence. We modified the *A. chinensis* genome into a consensus *A. arguta* genome by substituting the alternative homozygous variants of the female parent 'Ruby-3' using custom python scripts, to maximize the efficacy of the probes on the array. Sequencing reads were re-aligned and SNPs were identified from the modified 'Ruby-3' genome. We selected SNPs with 35 flanking nucleotides on both sides without additional SNPs or Indels. The resulting SNPs were quality filtered and only biallelic SNPs were kept. The flanking sequences of SNPs were extracted using a custom perl script and mapped back to the original *A. chinensis* genome using BLAST+(version 2.2.28). To maximize the likelihood that SNPs were polymorphic across *Actinidia* genotypes, the common SNPs from the subsets of the sequences: (1) polymorphic between the parents 'Ruby-3' and 'KuiLv-M' of the F1 population and (2) polymorphic among the kiwifruit accessions were selected for further technical assessment by Thermo Scientific Affymetrix platform and categorized into 'recommended', 'neutral' and 'not recommended'. The recommended SNPs were preferably included on the array, followed by neutral SNPs. To filter against multiple locations of probes in the genome, the probe sequences were aligned to the *A. chinensis* by BLASTN. SNPs with only 1 hit were selected and functionally annotated with putative impacts using SnpEff 4.2. Variants that were homozygous in both parents were removed as these are non-informative for linkage analysis. A/T and C/G polymorphisms were selected against, as these SNPs require twice the number of probes on the array. Genomic positions of SNPs were estimated in the *A. chinensis* genome and used in filtering of loci to ascertain an even distribution of marker loci across the genome to be included on the array. In total, 134 729 target sites were tiled in 6 micron square features on the chip.

Array evaluation

Genomic DNA was extracted from fresh leaves using the Plant DNA Extraction Kit (Tiangen Biotech Co., Ltd., Beijing, China). DNA sample was amplified, fragmented and hybridized on the chip followed by single-base extension through DNA ligation and signal amplification, following the Axiom 2.0 Assay Manual. The Axiom assay was performed on the Affymetrix GeneTitan system according to the user manual by the Beijing Compass Biotechnology Co., Ltd. (Beijing, China).

Following array hybridization and imaging, intensities of probe signals were processed in Axiom Analysis Suite. Genotypic data were filtered by MAF ≥5% and missing rates <0.1. MDS analysis was performed using PLINK v1.90 (Purcell *et al*., 2007). In addition, we evaluated the efficiency of genotyping polyploids by assigning allele dosage. Marker dosages were called from allele signal ratios of the array using fitPoly (Voorrips *et al*., 2011).

Linkage map construction

The F1 population of 'Ruby-3' × 'Kuilv-M' was genotyped to construct a linkage map using polymapR (Bourke *et al*., 2018a). Markers were filtered by assessing the match of parental dosage scores with the segregation of dosages in their progeny, by the expected tetraploid segregation ratios and by allowing no more than 10% missing scores. A principal components analysis was performed to exclude incompatible progenies from the dataset. Duplicates were merged as unique individuals. Redundant markers were marked and merged to reduce uninformative markers for linkage calculations. Marker dosages were converted into nine simplest segregation types.

The recombination frequency (r), LOD scores and phasing of all marker pairs were calculated separately for each parent. The simplex × nulliplex and nulliplex × simplex markers in the coupling phase were tested to cluster markers into pseudo-homologues at LOD scores ranging from 4 to 12. The multi-dose markers such as the duplex × nulliplex or simplex × simplex markers were used to bridge homologues together, which creates the links between pseudo-homologue linkage groups. The biparental markers defined consensus numbers to the linkage groups between the parents. All other marker types were assigned to a linkage group and homologues using their linkage to simplex × nulliplex markers. The consistency of marker linkage group assignment was checked across parents. Markers with linkages to multiple linkage groups were removed before calculating all pairwise linkages for each marker combination within a linkage group. An integrated map of all linkage groups was created after map ordering using the MDSMap software (Preedy and Hackett, 2016). The previously binned markers (*i.e.* duplicates) were added back and markers were phased using the inbuilt phasing functionality of polymapR to generate a phased parental linkage map. The flanking sequence of markers was blasted against the *A. chinensis* genome. LGs were re-numbered and re-oriented to the expected physical position if necessary.

QTL mapping and estimation of preferential pairing

The F1 population of 'Ruby-3' × 'Kuilv-M' male was phenotyped visually for sex organs during flowering. QTL mapping was performed using functions in the package polyqtlR (Bourke *et al*., 2021). polyqtlR is a tool that performs QTL analysis using identity-by-descent (IBD) probabilities, which are the probabilities of inheritance of particular combinations of parental haplotypes. A LOD threshold for detecting significant QTL was calculated using a permutation test (1000 permutations, 95% threshold). Preferential pairing among parental homologues was diagnosed using the chromosomal pairing behaviour predicted by the Hidden Markov Model during IBD estimation in polyqtlR.

Acknowledgements

The authors thank Chengkui Qiao from Fruit and Nursery Stock Quality Supervision and Test Center (Zhengzhou) in our institute for assistance. We gratefully acknowledge the financial support from the National Key Research and Development Project of China (2019YFD1000802); Part of this research was funded under the TKI project: "Novel genetic and genomic tools for polyploid crops" (KV 1605-020; BO 26.03 009 004, BO 50 002 022) and USDA's National Institute of Food and Agriculture (NIFA) Speciality Crop Research Initiative project "Tools for genomics-assisted breeding in polyploids: Development of a community resource" (2020-51181-32156/SCRI). We also thank the National Natural Science Foundation of China (32001995) and the Special Engineering Science and Technology Innovation, Chinese Academy of Agricultural Sciences (CAAS-ASTIP-2015-ZFRI).

Conflicts of interest

The authors declare no conflicts of interest.

Authors' contributions

R.W. collected samples and drafted the manuscript. R.W., S.X. and P.M.B. carried out data analysis and manuscript editing. X.Q., M.L., H.G., Y.Z., Y.L., S. L. and L.S. contributed to the materials and technical guidance. D.E., P.A. and R.E.V. provided advice in SNP array design, dosage calling and manuscript editing. J.F., C.M. and R.V. conceived, designed and supervised the study.

Reference

Akagi, T., Pilkington, S.M., Varkonyi-Gasic, E., Henry, I.M., Sugano, S.S., Sonoda, M., Firl, A. *et al*. (2019) Two Y-chromosome-encoded genes determine sex in kiwifruit. *Nat. Plants* **5**, 801–809.

Allen, A.M., Winfield, M.O., Burridge, A.J., Downie, R.C., Benbow, H.R., Barker, G.L.A., Wilkinson, P.A. *et al*. (2017) Characterization of a wheat breeders' Array suitable for high-throughput SNP genotyping of global accessions of hexaploid bread wheat (*Triticum aestivum*). *Plant Biotechnol. J.* **15**, 390–401.

Bajgain, P., Rouse, M.N. and Anderson, J.A. (2016) Comparing genotyping-by-sequencing and single nucleotide polymorphism chip genotyping for quantitative trait loci mapping in wheat. *Crop. Sci.* **56**, 232–248.

Bassil, N.V., Davis, T.M., Zhang, H.L., Ficklin, S., Mittmann, M., Webster, T., Mahoney, L. *et al*. (2015) Development and preliminary evaluation of a 90 K Axiom® SNP array for the allo-octoploid cultivated strawberry Fragaria × ananassa. *BMC Genomics* **16**, 1–30.

Bourke, P.M., Hackett, C.A., Voorrips, R.E., Visser, R.G.F. and Maliepaard, C. (2019) Quantifying the power and precision of QTL analysis in autopolyploids under bivalent and multivalent genetic models. *G3 (Bethesda)* **9**, 2107–2122.

Bourke, P.M., van Geest, G., Voorrips, R.E., Jansen, J., Kranenburg, T., Shahin, A., Visser, R.G.F. *et al*. (2018a) polymapR-linkage analysis and genetic map construction from F1 populations of outcrossing polyploids. *Bioinformatics* **34**, 3496–3502.

Bourke, P.M., Voorrips, R.E., Hackett, C.A., van Geest, G., Willemsen, J.H., Arens, P., Smulders, M.J.M. *et al*. (2021) Detecting quantitative trait loci and exploring chromosomal pairing in autopolyploids using polyqtlR. *Bioinformatics* **37**, 3822–3829.

Bourke, P.M., Voorrips, R.E., Visser, R.G.F. and Maliepaard, C. (2018b) Tools for genetic studies in experimental populations of polyploids. *Front. Plant Sci.* **9**, 513.

Chagne, D., Crowhurst, R.N., Troggio, M., Davey, M.W., Gilmore, B., Lawley, C., Vanderzande, S. *et al*. (2012) Genome-wide SNP detection, validation, and development of an 8K SNP array for apple. *Plos One* **7**, e31745.

Ferguson, A.R. (2013) Kiwifruit: the wild and the cultivated plants. *Adv. Food Nutr. Res.* **68**, 15–32.

Fraser, L.G., Tsang, G.K., Datson, P.M., De Silva, H.N., Harvey, C.F., Gill, G.P., Crowhurst, R.N. *et al*. (2009) A gene-rich linkage map in the dioecious species *Actinidia chinensis* (kiwifruit) reveals putative X/Y sex-determining chromosomes. *BMC Genomics* **10**, 1–15.

Gerard, D., Ferrao, L.F.V., Garcia, A.A.F. and Stephens, M. (2018) Genotyping polyploids from messy sequencing data. *Genetics* **210**, 789–807.

Glick, L.S.N., Ashman, T., Emma, G. and Mayrose, I. (2016) Polyploidy and sexual system in angiosperms: Is there an association? *Am. J. Bot.* **103**, 1223–1235.

Hale, I., Melo, A.T.O. and Gustafson, H. (2018) Sex-linked molecular markers for two cold-hardy kiwifruit species, *Actinidia arguta* and *A. kolomikta*. *Eur. J. Hortic. Sci.* **83**, 236–246.

Huang, S.X., Ding, J., Deng, D.J., Tang, W., Sun, H.H., Liu, D.Y., Zhang, L. *et al*. (2013) Draft genome of the kiwifruit *Actinidia chinensis*. *Nat. Commun* **4**, 1–9.

Koning-Boucoiran, C.F., Esselink, G.D., Vukosavljev, M., van't Westende, W.P., Gitonga, V.W., Krens, F.A., Voorrips, R.E. *et al*. (2015) Using RNA-Seq to assemble a rose transcriptome with more than 13,000 full-length expressed genes and to develop the WagRhSNP 68k Axiom SNP array for rose (*Rosa* L.). *Front. Plant Sci.* **6**, 249.

Li, X., Singh, J., Qin, M., Li, S., Zhang, X., Zhang, M., Khan, A. *et al*. (2019) Development of an integrated 200K SNP genotyping array and application for genetic mapping, genome assembly improvement and genome wide association studies in pear (Pyrus). *Plant Biotechnol. J.* **17**, 1582–1594.

Liu, Y.F., Li, D.W., Zhang, Q., Song, C., Zhong, C.H., Zhang, X.D., Wang, Y. *et al*. (2017) Rapid radiations of both kiwifruit hybrid lineages and their parents shed light on a two-layer mode of species diversification. *New Phytol.* **215**, 877–890.

Pakull, B., Groppe, K., Mecucci, F., Gaudet, M., Sabatti, M. and Fladung, M. (2011) Genetic mapping of linkage group XIX and identification of sex-linked SSR markers in a Populus tremula × Populus tremuloides cross. *Can. J. For. Res.* **41**, 245–253.

Paolucci, I., Gaudet, M., Jorge, V., Beritognolo, I., Terzoli, S., Kuzminsky, E., Muleo, R. *et al*. (2010) Genetic linkage maps of *Populus alba* L. and comparative mapping analysis of sex determination across Populus species. *Tree Genet. Genomes* **6**, 863–875.

Peace, C., Bassil, N., Main, D., Ficklin, S., Rosyara, U.R., Stegmeir, T., Sebolt, A. *et al*. (2012) Development and evaluation of a genome-wide 6K SNP array for diploid sweet cherry and tetraploid sour cherry. *PLoS One* **7**, e48305.

Pilkington, S.M., Crowhurst, R., Hilario, E., Nardozza, S., Fraser, L., Peng, Y.Y., Gunaseelan, K. *et al*. (2018) A manually annotated *Actinidia chinensis* var. chinensis (kiwifruit) genome highlights the challenges associated with draft genomes and gene prediction in plants. *BMC Genom.* **19**, 1–19.

Popowski, E., Thomson, S.J., Knabel, M., Tahir, J., Crowhurst, R.N., Davy, M., Foster, T.M. *et al*. (2021) Construction of a high density genetic map for hexaploid kiwifruit (*Actinidia chinensis* var. *deliciosa*) using genotyping by sequencing. *G3 (Bethesda)* **11**, jkab142.

Preedy, K.F. and Hackett, C.A. (2016) A rapid marker ordering approach for high-density genetic linkage maps in experimental autotetraploid populations using multidimensional scaling. *Theoretical and Applied Genetics*, **129**, 2117–2132.

Purcell, S., Neale, B., Todd-Brown, K., Thomas, L., Ferreira, M.A.R., Bender, D., Maller, J. *et al*. (2007) PLINK: A tool set for whole-genome association and population-based linkage analyses. *Am. J. Hum. Genet.* **81**, 559–575.

Renner, S.S. (2014) The relative and absolute frequencies of angiosperm sexual systems: Dioecy, monoecy, gynodioecy, and an updated online database. *Am. J. Bot.* **101**, 1588–1596.

Scaglione, D., Fornasiero, A., Pinto, C., Cattonaro, F., Spadotto, A., Infante, R., Meneses, C. *et al*. (2015) A RAD-based linkage map of kiwifruit (*Actinidia chinensis* Pl.) as a tool to improve the genome assembly and to scan the genomic region of the gender determinant for the marker-assisted breeding. *Tree Genet. Genomes* **11**, 1–10.

Serang, O., Mollinari, M. and Garcia, A.A.F. (2012) Efficient exact maximum a posteriori computation for bayesian SNP genotyping in polyploids. *Plos One* **7**, e30906.

Tahir, J., Brendolise, C., Hoyte, S., Lucas, M., Thomson, S., Hoeata, K., McKenzie, C. *et al*. (2020) QTL mapping for resistance to cankers induced by *Pseudomonas syringae* pv. *actinidiae* (Psa) in a Tetraploid *Actinidia chinensis* Kiwifruit population. *Pathogens* **9**, 967.

Tahir, J., Crowhurst, R., Deroles, S., Hilario, E., Deng, C.C.L., Schaffer, R., Le Lievre, L. *et al*. (2022) First chromosome-scale assembly and deep floral-bud transcriptome of a male Kiwifruit. *Front. Genet.* **13**, 961.

Tahir, J., Hoyte, S., Bassett, H., Brendolise, C., Chatterjee, A., Templeton, K., Deng, C. *et al*. (2019) Multiple quantitative trait loci contribute to resistance to bacterial canker incited by *Pseudomonas syringae* pv. actinidiae in kiwifruit (*Actinidia chinensis*). *Hortic. Res.* **6**, 101.

Tennessen, J.A., Wei, N., Straub, S., Govindarajulu, R., Liston, A. and Ashman, T.L. (2018) Repeated translocation of a gene cassette drives sex-chromosome turnover in strawberries. *PLoS Biol.* **16**, e2006062.

Testolin, R., Huang, H.W. and Ferguson, A.R. (2016) *The Kiwifruit Genome*. Berlin, Germany: Springer.

Testolin, R., Huang, W.G., Lain, O., Messina, R., Vecchione, A. and Cipriani, G. (2001) A kiwifruit (*Actinidia* spp.) linkage map based on microsatellites and integrated with AFLP markers. *Theor. Appl. Genet.* **103**, 30–36.

Uitdewilligen, J.G., Wolters, A.M., D'Hoop, B.B., Borm, T.J., Visser, R.G. and Van Eck, H.J. (2013) A next-generation sequencing method for genotyping-by-sequencing of highly heterozygous autotetraploid potato. *PLoS One* **8**, e62355.

Van Geest, G., Voorrips, R.E., Esselink, D., Post, A., Visser, R.G. and Arens, P. (2017) Conclusive evidence for hexasomic inheritance in chrysanthemum based on analysis of a 183 k SNP array. *BMC Genomics* **18**, 585.

Verde, I., Bassil, N., Scalabrin, S., Gilmore, B., Lawley, C.T., Gasic, K., Micheletti, D. *et al*. (2012) Development and evaluation of a 9K SNP array for peach by internationally coordinated SNP detection and validation in breeding germplasm. *PLoS One* **7**, e35668.

Voorrips, R.E., Gort, G. and Vosman, B. (2011) Genotype calling in tetraploid species from bi-allelic marker data using mixture models. *BMC Bioinform.* **12**, 1–11.

Vos, P.G., Uitdewilligen, J.G.A.M.L., Voorrips, R.E., Visser, R.G.F. and van Eck, H.J. (2015) Development and analysis of a 20K SNP array for potato (*Solanum tuberosum*): an insight into the breeding history. *Theor. Appl. Genet.* **128**, 2387–2401.

Vukosavljev, M., Arens, P., Voorrips, R.E., van't Westende, W.P.C., Esselink, G.D., Bourke, P.M., Cox, P. *et al*. (2016) High-density SNP-based genetic maps for the parents of an outcrossed and a selfed tetraploid garden rose cross, inferred from admixed progeny using the 68k rose SNP array. *Hortic. Res.* **3**, 16052.

Wei, N., Govindarajulu, R., Tennessen, J.A., Liston, A. and Ashman, T.L. (2017) Genetic mapping and phylogenetic analysis reveal intraspecific variation in sex chromosomes of the virginian strawberry. *J. Hered.* **108**, 731–739.

Winfield, M.O., Allen, A.M., Burridge, A.J., Barker, G.L.A., Benbow, H.R., Wilkinson, P.A., Coghill, J. *et al*. (2016) High-density SNP genotyping array for hexaploid wheat and its secondary and tertiary gene pool. *Plant Biotechnol. J.* **14**, 1195–1206.

Wu, J.H., Ferguson, A.R., Murray, B.G., Jia, Y.L., Datson, P.M. and Zhang, J.L. (2012) Induced polyploidy dramatically increases the size and alters the shape of fruit in *Actinidia chinensis*. *Ann. Bot.* **109**, 169–179.

You, Q., Yang, X.P., Peng, Z., Xu, L.P. and Wang, J.P. (2018) Development and applications of a high throughput genotyping tool for polyploid crops: Single nucleotide polymorphism (SNP) array. *Front. Plant Sci.* **9**, 104.

Zhang, Q., Liu, C.Y., Liu, Y.F., VanBuren, R., Yao, X.H., Zhong, C.H. and Huang, H.W. (2015) High-density interspecific genetic maps of kiwifruit and the identification of sex-specific markers. *DNA Res.* **22**, 367–375.

Zhang, Y., Zhong, C., Liu, Y., Zhang, Q., Sun, X. and Li, D. (2017) Agronomic trait variations and ploidy differentiation of kiwiberries in Northwest China: Implication for breeding. *Front. Plant Sci.* **8**, 711.

Zych, K., Gort, G., Maliepaard, C.A., Jansen, R.C. and Voorrips, R.E. (2019) FitTetra 2.0 - improved genotype calling for tetraploids with multiple population and parental data support. *BMC Bioinform.* **20**, 148.

Supporting information

Additional supporting information may be found online in the Supporting Information section at the end of the article.

Figure S1 Marker segregation summary of the tetraploid *A. arguta* population dataset.
Figure S2 Comparison of LG3 and LG25 between previously published diploid *A. chinensis* linkage map and the tetraploid *A. arguta* integrated linkage map.
Figure S3 Distribution of markers on LG3 of the integrated linkage map.
Figure S4 QTL analysis of the sex locus.
Figure S5 The IBD haplotype profiles of nine offspring for LG3.
Figure S6 Genotypic information Coefficient (GIC) plots for 29 linkage groups.

Table S1 Summary of materials used for sequencing and array evaluation.
Table S2 Sequencing summary of all *Actinidia* individuals.
Table S3 Chromosome pairing predictions during parental meiosis as estimated by polyqtlR.